STUDY OF A SPACE ROBOT CAPTURING A FAST ROTATING OBJECT FROM A FLOATING SPACECRAFT

*Shuang Wu[1], Fangli Mou[2], Ou Ma[3], Dapeng Han[4]

[1]*Department of Aeronautics & Astronautics Engineering, Tsinghua University, Beijing 100084, China, E-mail: wushuang11@mail.tsinghua.edu.cn*

[2]*Department of Automation, Tsinghua University, Beijing 100084, China,E-mail: mfl15@mails.tsinghua.edu.cn*

[3]*Department of Mechanical and Aerospace Engineering, New Mexico State University, Las Cruces, NM 88003, USA, E-mail: oma@mail.tsinghua.edu.cn*

[4]*Department of Aeronautics & Astronautics Engineering, Tsinghua University, Beijing 100084, China, E-mail: dphan@foxmail.com*

ABSTRACT

Capturing a target object in orbit is very difficult when the object is fast rotating. In this paper, the robot control strategy and the corresponding contact dynamics behavior of the vehicle-robot system are investigated in order to capture a fast rotating object. A nonlinear frictional contact model is proposed to represent the frictional and multiple-point contact phenomenon of the robotic capture problem. The control strategy of the capture operation is a combination of a resolved motion rate control (RMRC) method and an impedance control method, whose control goal is to reduce the relative velocity at the contact spots and increase the compliance of the arm during the pre-capture contacting period. A simulation example of a 3-joint manipulator reaching and capturing a rotating target object is provided to demonstrate the effectiveness of the proposed control method and the contact dynamics modeling and simulation method. The simulation example shows that the proposed control strategy performed very well for the capture of an object having an initial rotation speed of 10 deg/s (1.67 rpm).

1 INTRODUCTION

Space robots have been successfully used in many applications for on-orbit services, for instance, assembling and maintaining the International Space Station, repairing the Hubble telescope, and deploying/retrieving satellites in orbit. However, more complex and risky robotic tasks, such as to capture a fast rotating satellite or a piece of orbital junk, require more research work before they can be implemented in the future on-orbit service missions. This paper describes a research project at Tsinghua University to study a space robot capturing a fast rotating object in orbit.

A robotic task of capturing a rotating object for on-orbit service may be broken down into four phases: (1) keep the servicing vehicle in station keeping to observe the target object and plan the capture strategy; (2) control the robot to approach the object while regulating the attitude of the servicing vehicle; (3) grasp the target object without destabilization of the servicing vehicle; and (4) suppress the rotational motion of the post-capture combined system including both the servicing vehicle and the target object. The recent studies reported in the literature focused mostly on the second and fourth phases where robot control algorithms were developed and studied. In fact, the third phase is the most critical operation of the entire capture task but most of the published papers skip this critical part by assuming it as an instant event as opposed to a contact dynamic process. In fact, the grasping phase can run from a few seconds to minutes depending on the nature of the involved robot and the target as well as their relative motion condition. In this paper, the study is mainly focused on the third phase of a robotic capture task, which is to study the control strategy for capturing and the corresponding contact dynamics behavior of the capturing process, assuming the physical contact interfaces having complex geometry.

Contact between a space manipulator and a target object is a complicated nonlinear dynamic process. A high-fidelity and accurate contact model usually needs to be constructed for developing and verifying the performance of the capture control. So far, a number of contact dynamics modeling methods have been proposed in the literatures, which can be classified into two categories: discrete and continuous [1]. The discrete approach, also referred to as impulse-momentum approach [2], assumes that the contact between the objects occurs in a short time and that the configuration of contacting bodies do not change significantly. This approach models the impact between rigid bodies. The extension to flexible systems and generic multi-body systems is quite complicated. The continuous approach, also

referred to as force based approach or compliance contact modeling approach [2], models the impact force as a function of local indentation. This approach is suitable for the study of the impact with multiple contact points. In this approach, the spring-dashpot model [3] is simple but not physically realistic. Hertz's model [4] is the first nonlinear continuous contact model, which represents the relationship between the impact force and the indentation. Then Hunt and Crossley [5] introduce a nonlinear damping term to the Hertz's model. In recent years, Liu et al. [6] presented a new compliant force model for the contact problem of cylindrical joints with clearances. Luo and Nahon [7] extended the Hertz contact method for polyhedral contacting objects. The compliance contact model can offer the highest modeling fidelity and can be widely applied to complex contact interfaces and arbitrary contact motions. So the compliance contact modeling approach was applied in this study to model the contact force between the space robot and the rotating object. In addition, the 3-D bristle contact friction modeling method [8] was introduced to represent the friction phenomenon during the contact.

Appropriate design of control strategy is vital for the success of robot capture, especially when capturing at a large relative speed. Since Hogan first proposed the impedance control methodology for robot contact-motion control in 1985 [9], tremendous studies have been done to improve and advance this control method. To date, impedance control and its derivatives are still known as the most effective control methods for handling robot contact problems. Yoshida et al. [10] first applied the impedance control method to the problem of a space robot performing contact tasks. Ma et al. [11] employed impedance control to protect manipulators from bending and twisting due to contact force in a capturing process. However, these existing studies only dealt with simple contact and non-rotational robotic capture problems. In our study, a derivative of the impedance control, admittance control method, was combined with the resolved motion rate control (RMRC) [12] to solve a more challenging robotic capture problem characterized with rotational motion and complex contact geometry.

In this paper, a nonlinear frictional contact model is proposed to represent the nonlinear contact and friction phenomena during the target capture. And an RMRC and impedance control combined control strategy is designed for the complex robotic capture problem, which can reduce the contact force and realize the good tracking control simultaneously. A simulation example of a 3-joint manipulator capturing a rotating target object is developed to demonstrate the feasibility and effectiveness of the proposed frictional contact model and the innovated robotic capture control strategy.

2 CONTACT DYNAMICS MODELING

2.1 Dynamic Model of a Space Robot

For an n-DOF free-floating space robot when it operates in space, its dynamics is governed by the following equation:

$$\boldsymbol{D}(\boldsymbol{q})\ddot{\boldsymbol{q}} + \boldsymbol{C}(\boldsymbol{q},\dot{\boldsymbol{q}})\dot{\boldsymbol{q}} + \boldsymbol{g}(\boldsymbol{q}) + \boldsymbol{\tau}_f(\dot{\boldsymbol{q}}) = \boldsymbol{\tau} + \boldsymbol{\tau}_{ext} \quad (1)$$

where $\boldsymbol{q}$ is the vector of generalized coordinates which are joint angles of the space robot; $\boldsymbol{D}$ is the generalized inertia matrix which is an nonlinear function of joint coordinates $\boldsymbol{q}$; $\boldsymbol{C}$ is the centripetal and Coriolis vector depending on the joint coordinates $\boldsymbol{q}$ and joint rates $\dot{\boldsymbol{q}}$; $\boldsymbol{g}$ is the gravity torque vector depending on the joint coordinates $\boldsymbol{q}$; $\boldsymbol{\tau}$ represents the generalized forces vector applied on the joints of the space robot; vectors $\boldsymbol{\tau}_f$ and $\boldsymbol{\tau}_{ext}$ are respectively the joint friction torques and the torques due to external forces applied on the robot.

2.2 Contact Dynamics Model

2.2.1 Nonlinear spring-damping contact model

The compliance contact modeling method that describes the continuous contact dynamics is used here to model the contact force between the space manipulator and the fast rotating target object.

The compliance method models each contact region or point as a spring-damping model. Combining the Hertz's model [4] with the nonlinear damping [5], the normal contact/impact force can be modeled as a nonlinear spring-damping system:

$$\boldsymbol{F}_n = b\delta\dot{\delta}\boldsymbol{n} + k\delta^{3/2}\boldsymbol{n} \quad (2)$$

where δ and $\boldsymbol{n}$ present the local indentation and the unit surface normal vector at the contact point, respectively; b and k are damping parameter and contact stiffness, respectively, which are defined as

$$b = 2\zeta\sqrt{k\frac{m_1 m_2}{m_1 + m_2}} \quad (3)$$

$$k = c\frac{E_1 E_2}{E_1\left(1-\upsilon_2^2\right) + E_2\left(1-\upsilon_1^2\right)}a \quad (4)$$

$$a = \sqrt{A/\pi} \quad (5)$$

$$\frac{4}{3} \le c \le 2\pi \quad (6)$$

where ζ represents the material damping coefficient; m_1 and m_2 are the masses of the two contacting bodies, respectively; c is surface loading

coefficient; E_1 and E_2 are Younge's modulus of the two bodies; υ_1 and υ_1 are the Poission's ratios of the two bodies; A is contacting surface area and a is the contact radius of the contact surface area A.

2.2.2 Nonlinear friction force model

Friction that exists in contact between a space manipulator and a rotating target object is a complicated nonlinear phenomenon caused by interactions between contacting surfaces. It influenced by not only the motion state of the two contacting bodies but also materials, geometry, temperature, moisture and so on. Since the friction has an effect on the contact dynamics so as to slow or stop the capture operation, an accurate friction force model is required for contact dynamics analysis during the capture.

Bristle friction force models have been used by many researchers as a preferred method for friction forces modeling. This model can represents the physical reality for some practical application cases. A 3-dimensional bristle friction force model [8] is used to describe the friction forces of the two contacting bodies in the process of capture. The expression of the model is as follows:

$$\boldsymbol{F}_t = -k_b \mathbf{s} - c_b \dot{\mathbf{s}} \tag{7}$$

$$\mathbf{s}(t) = \begin{cases} \mathbf{s}(t_0) + \int_{t_0}^{t} \mathbf{v}_t(t)\,dt & \text{if } |\mathbf{s}| < s_{\max}(t) \\ s_{\max}(t)\dfrac{\mathbf{v}_t(t)}{|\mathbf{v}_t(t)|} & \text{if } |\mathbf{s}| \geq s_{\max}(t) \end{cases} \tag{8}$$

where k_b is bristle stiffness; c_b is bristle damping coefficient; $\mathbf{s}$ is average bristle deflection or displacement; t_0 is starting time; t is current time; $\mathbf{v}_t$ is tangential velocity between the two contacting bodies at the contact point. $s_{\max}$ is maximum bristle deflection.

3 ROBOT CONTROL DESIGN

The key of a general capture process is to design a control strategy for the approaching and grasping phases. In approaching phase, our goal is to move the robot gripper to an ideal pose such that when the gripper touches the capture structure of the target, zero or a very small impact force will result from the initial contact between the gripper and the capture structure. Hence, the control goal of this phase would be to achieve zero relative velocity between the gripper and the capture structure at the initial contact. In the subsequent grasping phase, the gripper continues to move trying to cover the capture structure with its opening end as much as possible so that the rotating object can be successfully captured when the gripper closes. The goal of the control strategy in this phase is to not only reach the successful catch depth but also cause as little contact force as possible between the gripper and the capture structure.

3.1 Control Strategy

A combined control strategy is presented for approaching and grasping the target object. It consists of a resolved motion rate controller, an impedance controller and a contact discriminant module. The resolved motion rate controller is performed throughout the whole approaching and grasping processes. The design objective of the resolved motion rate controller is to achieve both fast and accurate tracking for the rotating object. The impedance controller is performed when contact occurs, and the design goal of the impedance controller is to minimize the contact forces between the gripper and the capture structure. It is worthy to note that a contact discriminant module is designed for the impedance controller, which is used to determine when the control system should perform impedance control. The Block diagram of the combined control strategy is shown in Figure 1.

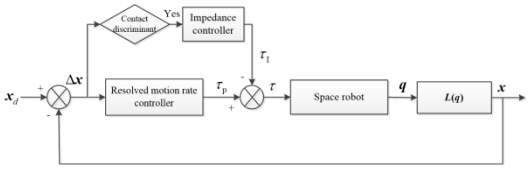

Figure 1: Block diagram of the combined control strategy.

3.2 Control Law

3.2.1 Resolved motion rate controller

Generally, the kinematic relationship between the Cartesian space and the joint space of a manipulator is given by

$$\boldsymbol{x}(t) = \boldsymbol{f}[\boldsymbol{q}(t)] \tag{9}$$

Their differential relationships are

$$\dot{\boldsymbol{x}}(t) = \boldsymbol{J}(\boldsymbol{q})\dot{\boldsymbol{q}}(t) \tag{10}$$

where $\boldsymbol{J}$ is the Jacobian matrix, evaluated at the current configuration $\boldsymbol{q}$.

The general solution of (10) using the pseudo-inverse is obtained as follows

$$\dot{\boldsymbol{q}}(t) = \boldsymbol{J}^{\#}(\boldsymbol{q})\dot{\boldsymbol{x}}(t) + [\boldsymbol{I}_n - \boldsymbol{J}^{\#}(\boldsymbol{q})\boldsymbol{J}(\boldsymbol{q})]\boldsymbol{y} \tag{11}$$

where $\boldsymbol{J}^{\#}(\boldsymbol{q})$ is the pseudo inverse of $\boldsymbol{J}(\boldsymbol{q})$; $\boldsymbol{I}_n$ is an identity matrix; and $\boldsymbol{y}$ is a vector in the null space of $\boldsymbol{J}$, which can be determined for an optimization need.

The manipulator joint torque vector to realize the desired motion trajectory is

$$\boldsymbol{\tau} = \boldsymbol{D}(\boldsymbol{q})\ddot{\boldsymbol{q}} + \boldsymbol{C}(\boldsymbol{q},\dot{\boldsymbol{q}})(\dot{\boldsymbol{q}}_d - \dot{\boldsymbol{q}}) + \boldsymbol{g}(\boldsymbol{q}) + \boldsymbol{\tau}_f(\dot{\boldsymbol{q}}) - \boldsymbol{\tau}_{ext} \quad (12)$$

where the desired joint rate vector $\dot{\boldsymbol{q}}_d(t)$ is

$$\dot{\boldsymbol{q}}_d(t) = \boldsymbol{J}^{\#}(\boldsymbol{q})\dot{\boldsymbol{x}}_d(t) + [\boldsymbol{I}_n - \boldsymbol{J}^{\#}(\boldsymbol{q})\boldsymbol{J}(\boldsymbol{q})]\boldsymbol{y} \quad (13)$$

3.2.2 Impedance controller

The goal of the impedance control is to construct a second-order mass-damper-spring relationship between end-effector position and contact force, so as to achieve a closed loop behavior which resembles a given impedance behavior [9]. The basic equation of the second-order dynamic relationship between end-effector position and contact force is given by:

$$\boldsymbol{M}\Delta\ddot{\boldsymbol{x}} + \boldsymbol{B}\Delta\dot{\boldsymbol{x}} + \boldsymbol{K}\Delta\boldsymbol{x} = \boldsymbol{F}_c \quad (14)$$

where $\boldsymbol{M}$, $\boldsymbol{B}$ and $\boldsymbol{K}$ are positive definite matrices representing the virtual inertia, damping and stiffness of the manipulator; $\boldsymbol{F}_c$ is the contact force between the manipulator end-effector and the target object. $\Delta\boldsymbol{x}$ and $\Delta\dot{\boldsymbol{x}}$ are the differences between the desired and the actual position and velocity of the manipulator end-point, which can be expressed in actuator coordinates

$$\Delta\boldsymbol{x} = \boldsymbol{x}_d - \boldsymbol{L}(\boldsymbol{q})$$
$$\Delta\dot{\boldsymbol{x}} = \dot{\boldsymbol{x}}_d - \boldsymbol{J}(\boldsymbol{q})\boldsymbol{w}$$

If contact forces are detected by contact discriminant module, the impedance controller will be carried out to revise the desired trajectory obtained from the resolved motion rate controller to reduce the contacting forces between the robot end-effector and the target object. The revised end-effector trajectory and velocity are as follows:

$$\boldsymbol{x}_d = \boldsymbol{L}(\boldsymbol{q}) + \Delta\boldsymbol{x}$$

$$\dot{\boldsymbol{x}}_d = \boldsymbol{J}(\boldsymbol{q})\boldsymbol{w} + \Delta\dot{\boldsymbol{x}}$$

The joint torques to realize such impedance characteristics are

$$\begin{aligned}\boldsymbol{\tau} = {} & \boldsymbol{D}(\boldsymbol{q})\boldsymbol{J}^{-1}\left[-\boldsymbol{M}^{-1}\left(\boldsymbol{B}(\dot{\boldsymbol{x}}_d - \boldsymbol{J}(\boldsymbol{q})\boldsymbol{w}) + \boldsymbol{K}(\boldsymbol{x}_d - \boldsymbol{L}(\boldsymbol{q}))\right)\right. \\ & \left. -\dot{\boldsymbol{J}}\dot{\boldsymbol{q}}\right] - \left[\boldsymbol{J}^{\boldsymbol{T}} - \boldsymbol{D}(\boldsymbol{q})\boldsymbol{J}^{-1}\boldsymbol{M}^{-1}\right]\boldsymbol{F}_c + \boldsymbol{C}(\boldsymbol{q},\dot{\boldsymbol{q}})\dot{\boldsymbol{q}} + \boldsymbol{g}(\boldsymbol{q}) \quad (15) \\ & + \boldsymbol{\tau}_f(\dot{\boldsymbol{q}})\end{aligned}$$

4 SIMULATION EXAMPLE

4.1 Simulation Model

A simulation example of controlling a robot to capture a freely moving and rotating object was designed to demonstrate the effectiveness of the proposed frictional contact model and the control strategy for capture. Figure 2 is an illustration of a 3-joint (3 degrees of freedom) manipulator capturing a rotating object in a 2D plane. The target object can freely rotate and translate in the 2D plane. Initially, the target object is purely rotating without translation because of no external forces applied on the target. Once the robot gripper touches the target, it will start translating and changing rotation because of the contact force from the touching. Therefore, it has to be very careful when controlling the robot to approach and grasp the object. The key of this work is to design an appropriate control strategy to control the robot from its initial configuration until completion of the capture task. In this example, perfect sensors are assumed for the robot controller and the target object is assumed rotating in the XY plane at an initial speed of ω.

The operation procedure for a robotic capture task can always be divided into the following four phases:

(1) Observing and planning phase: In the time before t_0, the robot is at rest and its gripper is at the P_0 configuration, as shown in Figure 2.

(2) Approaching phase: During the time from t_0 to t_1, the robot gripper is controlled to move from its initial configuration $\boldsymbol{P}_0$ to the impending-contact configuration $\boldsymbol{P}_1$.

In this phase, the control goal is to move the gripper to an ideal pose $\boldsymbol{P}_1$ such that, zero or a very small impact force will result from the initial contact between the gripper and the capture bar of the target (a straight rod on the target object for the robot gripper to catch). The motion trajectory of the gripper is traced by the blue curve in Figure 2.

(3) Grasping phase (soft-contact phase): During the time from t_1 to t_2, the robot gripper is controlled to move from the configuration $\boldsymbol{P}_1$ to the capture configuration $\boldsymbol{P}_2$.

In this phase, the gripper continues to move, trying to cover the capture bar with its opening end as much as possible so that the capture bar can be successfully captured when the gripper closes. It is assumed that, the gripper will be able to catch the capture bar if 3/4 of its length enters into the opening of the gripper. The motion trajectory of the gripper in this phase is shown in the red curve in Figure 2.

(4) Post-capture stabilization phase: For the time after t_2, suppress the translational and rotational motions of the post-capture combined system.

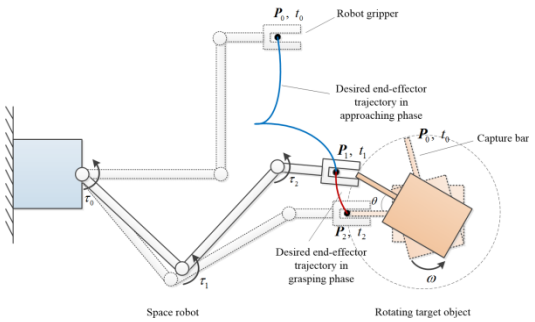

Figure 2: A 3-joint planar manipulator capturing a rotating target object.

The combined control strategy presented in Section 3 is used in the above-mentioned second and third phases of the capture operation. The first and the fourth phases are out of the scope of this paper and thus, will not be discussed here. The simulation of the dynamic robot control system is developed in MATLAB/Simulink environment with SimMechanics toolbox. The contact dynamics model is coded in M files and connected to the SimMechanics robot model through an S-function. The block diagram of the simulation system is shown in Figure 3.

As shown in Figure 3, the position and the attitude of the robot gripper and the capture bar are input into the contact dynamics model to compute contact forces and torques which are applied to the gripper and the bar in proper reference frames. Meanwhile, the contact forces and torques are also taken as inputs to the robot controller. The joint torques obtained from the controller are used to drive the robot joints. The block diagram of the combined controller is shown in Figure 4.

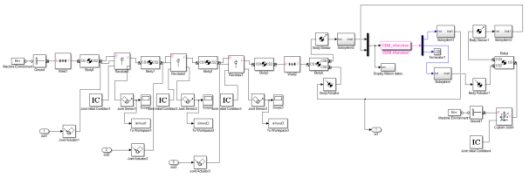

Figure 3: Block diagram of the simulation system for the robot to perform capturing task.

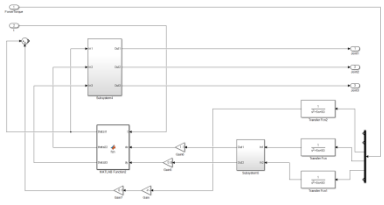

Figure 4: Block diagram of the combined robot controller.

4.2 Simulation Result

The target object is assumed free rotating in the XY plane at an initial speed of 10 deg/s (1.67 rpm). Figure 5 shows the relative position and attitude between the gripper and the target object. Figure 6 shows the contact forces and torques between the end-effector and the target object. Figure 7 shows the joint angles of the manipulator. In these figures, the dotted lines represent the results while using only RMRC for robot control, and the solid lines represent the results while using RMRC and impedance control combined control strategy. In these figures, the time from t_0=0 s to t_1=6.50 s is the approaching phase where the two different controllers generated almost the same results because of no contact in this phase. The time from t_1=6.50 s to t_2=9.63 s is the grasping phase and the first contact occurred at t_{c1}=7.06 s. As one can see from Figure 5, the relative position and attitude between the end-effector and the target object tended to be zero after the grasping phase, which indicates that a good target tracking can be achieved by the combined control strategy even after several bounces, and finally the capture task is accomplished successfully. Figure 6 shows that the contact forces and torques between the gripper and the target object are greatly reduced when applying the RMRC and impedance control combined strategy as opposed to just using the RMRC. Indeed, the latter did not achieve the capture goal because the capture bar was bounced away after a few moments of contacting. This example demonstrated that the proposed combined control strategy performs very well for capturing a fast rotating object.

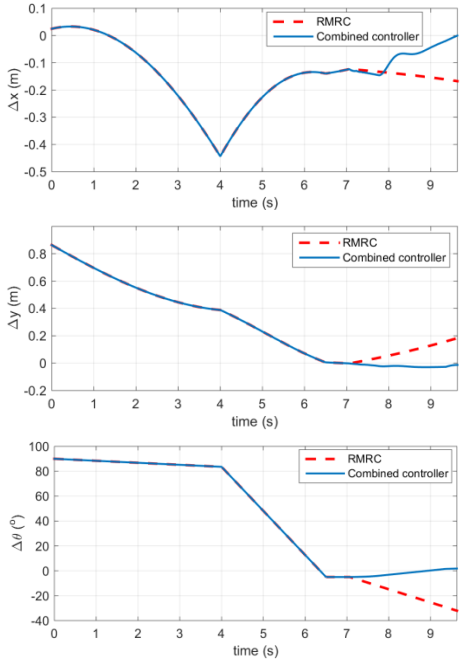

Figure 5: Relative position and attitude between the gripper and target object.

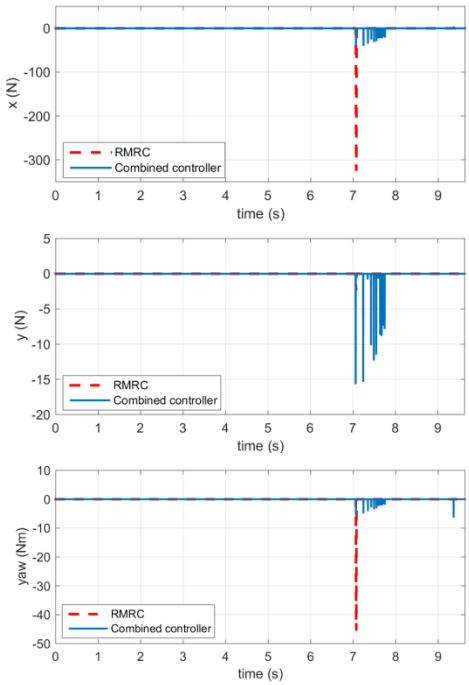

Figure 6: Contact forces and torques between the end-effector and the target object.

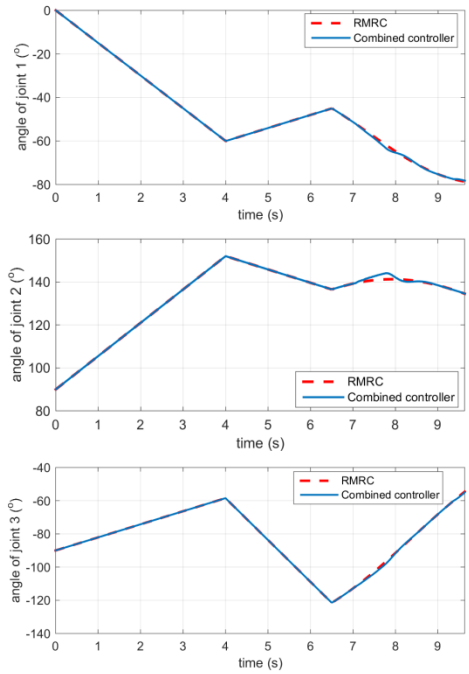

Figure 7: Joint trajectory of the manipulator.

5 CONCLUSION

This paper is concerned with the contact dynamics modeling and robot control strategy for capturing a fast rotating object. A compliance contact modeling method and bristle friction modeling method were used to establish a 3-dimensional, high-fidelity nonlinear frictional contact model. The proposed frictional contact model has high modeling fidelity to simulate arbitrary contact motions with complicated contact interfaces. Furthermore, the frictional behavior in both sliding and sticking regimes were also well simulated through this model. A combined control strategy was designed for the complex capture control problem. The presented control strategy can greatly reduce the contact forces at contact points as well as keeping both fast and good tracking for the rotating object. The effectiveness of the proposed contact dynamics model and the control strategy had been verified by a simulation example. The simulation results indicated that the goal of successfully capturing a fast rotating object using a robot was fulfilled well with the proposed control strategy, and the grasping operation was completed only within 3.2 seconds.

References

[1] Gilardi G and Sharf I (2002) Literature survey of contact dynamics modeling. *Mechanism and Machine Theory* 37(10):1213-1239.

[2] Kim SW (1999) *Contact dynamics and force control of flexible multi-body systems*. Doctoral Thesis, McGill University, Montreal, Quebec, Canada.

[3] Goldsmith W (1960) *Impact: The Theory and Physical Behavior of Colliding Solids*. Edward Arnold Publishers Ltd, London.

[4] Hertz H (1896) *Miscellaneous papers*. Macmillan, London.

[5] Hunt KH and Crossley FRE (1975) Coefficient of restitution interpreted as damping in vibroimpact. *Journal of Applied Mechanics* 42(2):440-445.

[6] Liu C, Zhang K and Yang L (2005) The compliance contact model of cylindrical joints with clearances. *Acta Mechanica Sinica* 21(5):451-458.

[7] Luo L and Nahon M (2011) Development and validation of geometry-based compliant contact models. *Journal of Computational and Nonlinear Dynamics* 6(1):011004.

[8] Liang J, Fillmore S and Ma O (2012) An extended bristle friction force model with experimental validation. *Mechanism and Machine Theory* 56:123-137.

[9] Hogan N (1985) Impedance control: an approach to manipulation, part i, ii, iii. *ASME Journal of Dynamic Systems, Measurement, and Control* 107(1):1-24.

[10] Yoshida K et al. (2004) Dynamics, control and

impedance matching for robotic capture of a non-cooperative satellite. *Advanced Robotics* 18(2):175-198.
[11] Ma G et al. (2015) Hand-eye servo and impedance control for manipulator arm to capture target satellite safely. *Robotica* 33(4):848-864.
[12] Whitney DE (1969) Resolved motion rate control of manipulators and human prostheses. *IEEE Transactions on Man-Machine Systems* 10(2):47-53.